

# Multipacting saturation in parallel plate and micro-pulse electron gun<sup>\*</sup>

LIAO Lang(廖浪)<sup>1,2;1)</sup> ZHANG Meng(张猛)<sup>1</sup> ZHAO Ming-Hua(赵明华)<sup>1;2)</sup><sup>1</sup> Shanghai Institute of Applied Physics, Chinese Academy of Sciences, Shanghai 201800, China<sup>2</sup> University of Chinese Academy of Sciences, Beijing 100049, China

**Abstract:** A novel parallel plate model is proposed that divides the electron cloud into three parts at saturation, and it is studied in detail using both an analytical approach and particle-in-cell (PIC) code simulations. As one part of the electron cloud, ribbons modes are suggested by tracking the trajectory of individual particles, and the aim of this mode form is to simplify the progress of the multipacting effect in the parallel plate so as to be eliminated by optimizing RF parameters. The micro-pulse electron gun (MPG) has demonstrated the potential to address the need for high peak and average current electron beams, hence studying the multipacting in MPG is essential. On the basis of studying multipacting in the parallel plate, it is clear that increasing the cavity voltage is of interest in yielding high quality beams in the gun.

**Key words:** multipacting, parallel plate, micro-pulse electron gun, electron source

**PACS:** 07.77.Ka, 79.20.Hx **DOI:** 10.1088/1674-1137/39/2/027003

## 1 Introduction

The multipacting can be initiated with primary electrons at the low energy region, and cause an avalanche by largely emitting secondary electrons in the cavity. Hence the multipacting is capable of disturbing the operation of RF structures, such as accelerator cavities and RF power couplers. Since the discovery of the phenomenon of multipacting in 1934 [1], it has been investigated both theoretically and experimentally in order to suppress it, in most cases [2–6]. Under specific circumstances, it was recognized as a new mechanism for the amplification of signals [7]. In 1993, multipacting was used in a micro-pulse electron gun (MPG) by taking advantage of its avalanche ability [8].

Previous investigations into multipacting are based on the Cu surface material, from which the average secondary yield  $\langle\delta\rangle$  shake was around 1 in the saturation stage [9, 10]. The steady state saturation is characterized by the fact that the number of electrons remains constant regardless of materials. With the required choice to have a gain of electrons in MPG with a grid-anode, the surface material is important. Previous studies show that MgO material is a good candidate because the maximum secondary emission yield (SEY) of MgO is higher than Cu [11]. Fig. 1 shows the secondary emission yield of MgO versus impact energy.

The parallel plate model is much more simple than any complexes. To get a better feeling for physics before studying factors to affect the mechanism of multipacting, a novel model which divides the electron cloud into three parts is proposed in the parallel plate as shown in Fig. 2. It then allowed us to investigate individual behavior of a particle by introducing a PIC code, i.e. VORPAL [12], which allows inclusion of the electromagnetic field and electron distribution minutia. Also a few examples of electron trajectories are presented to demonstrate the generation of hybrid resonance modes occurring in one simulation. Naturally, it is the goal of this part to have a better understanding of the multipacting effect.

Methods used to mitigate the effect of the hybrid modes are also discussed in order to improve the performance of MPG. For a single electron or a small group of electron beams, previous studies show that the emission phase would affect the arrival phase [13]. An important practical consideration is that multipacting in MPG will be initiated by a dark current, hence it is impossible to identify the initial phase for the initial electrons. In this case one can expect that the cavity voltage is used for optimization only. The cavity voltage is essential to the resonance of multipacting, and increasing cavity voltage leads to increasing the beam quality monitored at the exit of the anode—the details will be discussed later. Hence the cavity voltage is the one we can handle to

Received 9 April 2014

<sup>\*</sup> Supported by National Basic Research Program of China (973 Program) (2011CB808300) and National Natural Science Foundation of China (10935011)

1) E-mail: liaolang@sinap.ac.cn

2) E-mail: Corresponding author, zhaomh@sinap.ac.cn

©2015 Chinese Physical Society and the Institute of High Energy Physics of the Chinese Academy of Sciences and the Institute of Modern Physics of the Chinese Academy of Sciences and IOP Publishing Ltd

boost the energy high enough to balance the effect of the space charge force.

## 2 Parallel plate multipacting simulations

### 2.1 Parallel plate model

We consider the motion of electrons in the parallel plate model, from which a sinusoidal voltage of frequency  $\omega$  is applied to the gap with gap distance  $D$ . In this paper a sinusoidal-like transverse magnetic field is added in the parallel plate model, hence the situation is similar to the mode in the gun cavity and quite different from the studies before. As a sheet of initial electrons begins to traverse the gap, the competition of RF focusing and charge repulsion becomes more and more fierce. Until the balance of the charge repulsion and the RF focusing is achieved, the saturation stage seems to happen with the charge dispersion between the gap.

The parallel plate model we proposed here benefits from the study of multipacting Cu material [9, 10, 13, 14]. The difference of the multipacting effect between Cu and MgO material is mainly reduced to one factor: the secondary emission yield curve. The SEY curve, which describes the number of secondary electrons emitted per primary electron, was from Agarwal's work [15]. The SEY model for MgO material with a peak SEY of 20 at 1.5 keV impact energy is shown in Fig. 1. Here we are interested in the saturation stage of MgO material as opposed to the process of saturation, because the saturation stage plays a key role in gun performance.

In this model the wide bunch, as the result of saturation, is artificially divided into three parts. In reality, it is hard to make a distinction between these three parts, but we found that the schedule helps to avoid the influence of collective effects, thereby simplifying the analysis process. The electron cloud is assumed to be composed of three parts: (a) two-surface impact; (b) ribbon modes, as discussed in section 2.3; and (c) one-surface impact and ping-pong modes. Similar to the parallel plate model, these three parts also exist in the MPG, hence it is essential to discuss the influence in the gun cavity. Part (a) contributes to electron gain in the parallel plate as well as the MPG. Especially for MPG, the two-surface multipacting is mandatory to the phase focusing mechanism [4] which benefits the generation of micro-pulses. For part (c), the one-surface impact and ping-pong modes commonly exist during the process of multipacting, although it is undesirable in the gun. Ping-pong modes will increase the upper boundary of the multipacting region [14], which makes it hard to be eliminated in the cavity. But there is a possibility of improving the beam quality because of the existence of part (b). It is necessary to address part (b) because of its critical role in affecting the quality of beams and the details about this

part will given in section 2.3. The consideration of these three parts will help to give a better understanding of the process of multipacting, thereby helping to understand the plasma layer that prevents electrons from being extracted from material by the RF field [16]. Also this model may be the only way to explain the phenomenon, during high power tests for MPG, that the multipacting effect is dysfunctional at times [17].

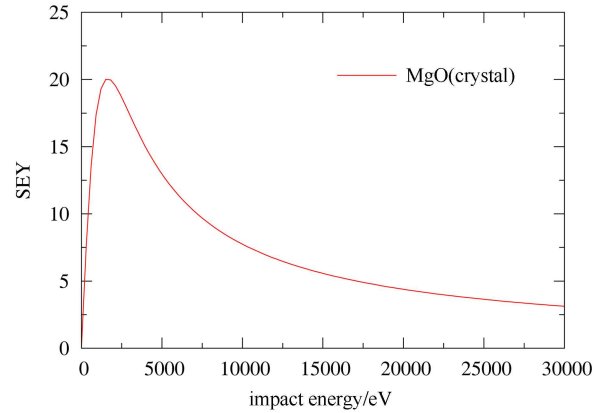


Fig. 1. Secondary emission yield curve for MgO crystal.

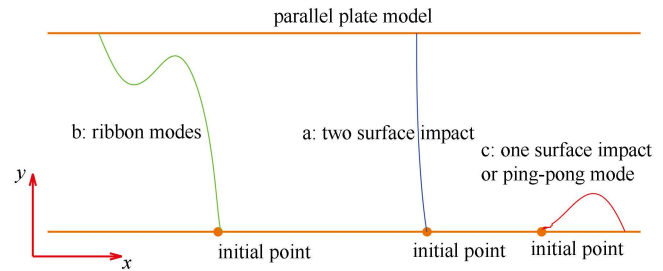


Fig. 2. A schematic drawing of a parallel plate multipacting model.

### 2.2 Particle tracking at saturation stage

Instead of investigating the collective effect at saturation, it is convenient to track each individual particle in the parallel plate. For the simulations here, after a slice of electrons emitted from one of the electrodes, it is only a small period for electrons growing to saturation between the parallel plate. Fig. 3 shows the phase space at the peak accelerating field of 6.5 MV/m at the given moment of time. An important thing to note from the figure is that the electrons disperse in the parallel plate, which is mainly because of the space charge effect. As a result of dispersion, the modes in the parallel plate become confused, which, of course, leads to bad understanding.

The trajectories of individual particles are shown in Fig. 4. The trajectories in the figure express the fact that at saturation lots of multipacting modes are concurrent in the parallel plate. Fig. 4 shows the one-surface, 1-st

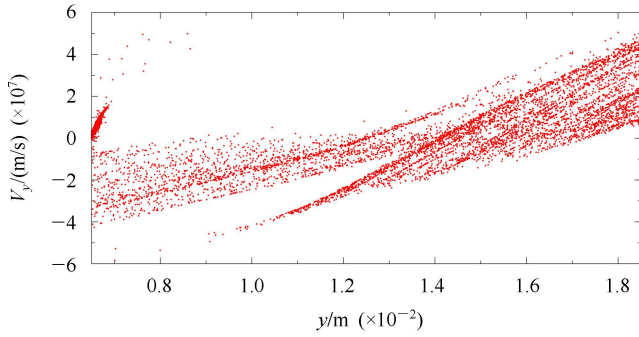


Fig. 3. Velocity in  $y$  direction versus  $y$  when the peak electric field  $E_0=6.5$  MV/m in the parallel plate at saturation.

order two-surface and higher order two-surface multipacting respectively. Also there is a new kind of multipacting mode as shown in Fig. 5. An electron is emitted from one electrode but it never hits another electrode. It seems that the electron is suspended in the space between the upper and lower plate. This kind of mode contributes to the formation of an electron cloud which is suspended in the free space. We found that 1-st order two-surface multipacting is common, which is needed for the running of the MPG; unfortunately the presence

of other modes would disturb the operation of the electron gun. In what follows, we suggest a resonant form to conclude this ‘suspension’ mode except from 1-st order two-surface multipacting and one-surface multipacting, and try to find a way to kick it out of the resonant condition.

### 2.3 Ribbon modes

Kishek has reported a kind of multipacting mode, namely ping-pong modes [14]. It may seem surprising that the ping-pong modes that combine one-surface and two-surface multipacting within a single period enhance the range of susceptibility of multipacting. In this case, the ping-pong modes extensively exist in the multipacting process. In this part, we will illustrate the ‘ribbon modes’ that combine higher order modes and suspension-like modes.

In what follows we ignore the space charge effect in our simulations. We assume that electrons emit from one electrode having an initial velocity  $v_0$  with an initial phase  $\varphi=\theta_0$ . The resonant electrons will traverse the gap at the phase of  $N\pi+\theta_0$ , thereby the resonance equation can be written as

$$y|_{\omega t=N\pi+\theta_0}=D. \quad (1)$$

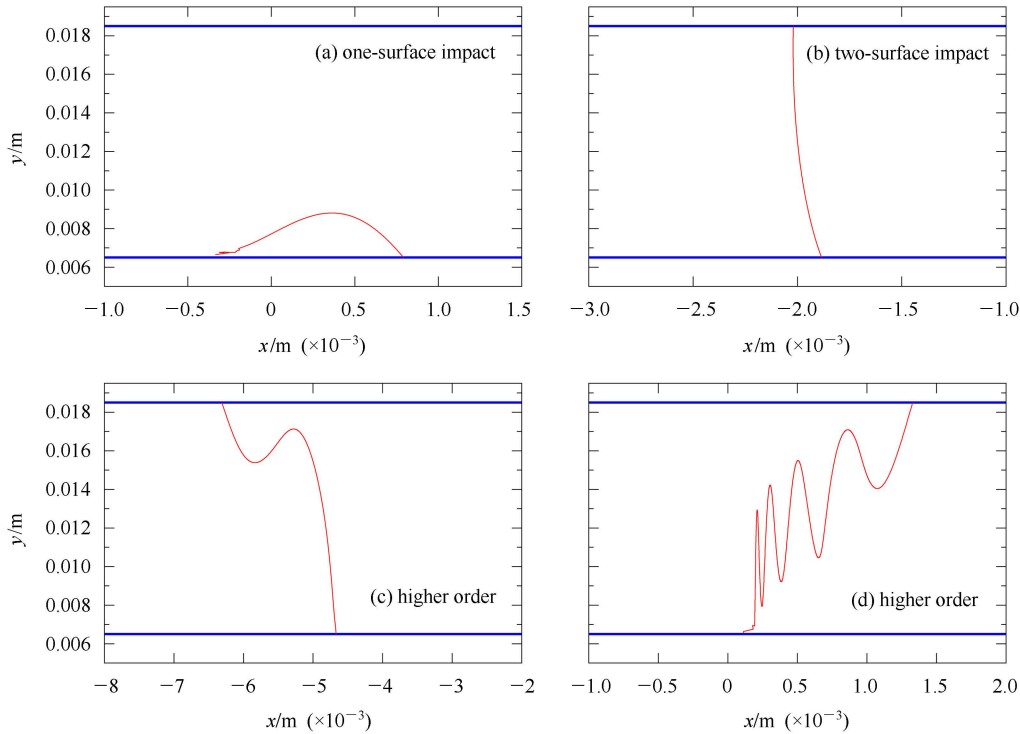


Fig. 4. Electron trajectories for different modes in the parallel plate at saturation, and the gap distance  $D=12.0$  mm. (a) One-surface multipacting; (b) 1-st order two-surface multipacting; (c) and (d) Higher order two-surface multipacting which belong to ribbon modes.

The situation was addressed in the crossed electric and magnetic fields, so the analytic solution of  $y$  in Eq. (1) can be replaced by Eq. (7a) from reference [9]. In this case, the quantity of  $\Omega$  is small enough to be ignored, hence Eq. (1) is easily calculated to be

$$\frac{V_{rf0}}{D} = \frac{m\omega[mD^2 - (N\pi + \theta_0)v_0]}{e[\sin(2\theta_0) + \sin\theta_0 + (N\pi + \theta_0)\cos\theta_0]}, \quad (2)$$

where  $m/e$  is the mass-charge ratio,  $V_{rf0}$  is the amplitude of the RF voltage and  $\omega = 2\pi f$  ( $f$  is the frequency of the cavity). Eq. (2) can be simplified by integrating the parameters from Table 1, and we have

$$E_0 = \frac{26.4 - 0.086(\pi + \theta_0)}{\sin(2\theta_0) + \sin\theta_0 + (\pi + \theta_0)\cos\theta_0} (\text{MV/m}). \quad (3)$$

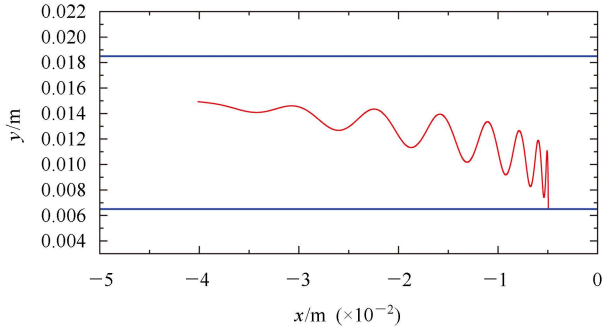


Fig. 5. A kind of electron trajectory in the parallel plate at saturation. The electron is emitted from one electrode and attempts to traverse the space. Obviously it will never hit another electrode, and it seems likely that the electron ‘floats’ in the free space.

Table 1. Parameters used to calculate Eq. (2).

parameters	value
frequency $f/\text{GHz}$	2.856
gap distance $D/\text{cm}$	1.2
initial energy $E_{ini}/\text{eV}$	2
order of multipacting $N$	1

Where  $E_0$  is the axis electric field in the cavity and the relations between  $E_0$  and initial phase  $\theta_0$  is drawn in Fig. 6. Actually, a fraction of electrons will hit the opposite electrode at the unresonance condition. As the electrons hit the electrode before the electric field can be reversed, 1-st order two-surface multipacting occurs in the model, and this condition corresponds to the trajectory shown in Fig. 7(a) and (b). But it should be noted that the electrons that traverse the gap after the electric field is reversed will have different trajectories. In this case, Eq. (3) becomes

$$E_0 < \frac{26.4 - 0.086(\pi + \theta_0)}{\sin(2\theta_0) + \sin\theta_0 + (\pi + \theta_0)\cos\theta_0} (\text{MV/m}). \quad (4)$$

The electrons which meet the requirement of Eq. (4) will yield ribbon-like trajectories as illustrated in Fig. 7(c), so we termed a series of these modes as ‘ribbon modes’. The A, B and C in Fig. 6 represent electron trajectories corresponding to Fig. 7(a), (b) and (c) respectively. Actually, the behavior of A, B and C particles is easy to be predict by Eq. (3) and in turn show a good agreement with Eq. (3).

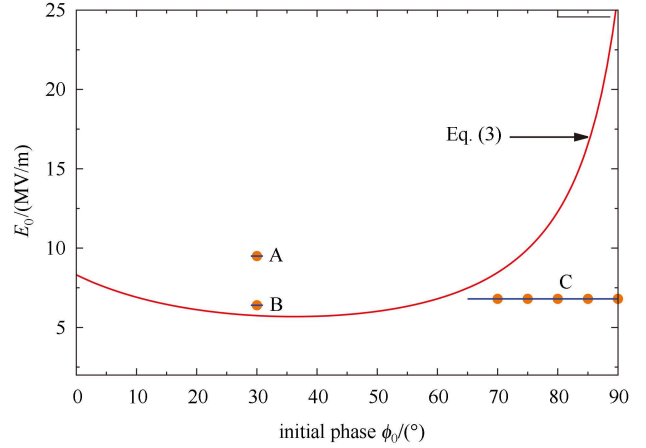


Fig. 6. Drawing of Eq. (2) at the range of  $[0, 90]$  degrees. Point A represents the electron emitted off the electrode with an initial phase of  $30^\circ$  at the electric field of 9.5 MV/m. Point B represents the electron emitted with an initial phase of  $30^\circ$  at the electric field of 6.4 MV/m. Area C represents the electron at the electric field of 6.8 MV/m for different initial phases.

Let us now consider the behavior of the ribbon modes. From Fig. 7(c) it is clear that the ribbon modes not only contain the higher order multipacting electrons, but also the electrons which will never hit the opposite electrode but are suspended in the free space of the cavity. At the given moment of time when the resonance electrons hit the opposite electrode, unresonance electrons still ‘float’ in the free space, just like a sheet of electron cloud. According to the phase focusing mechanisms as described in Ref. [4], some particles launched at some phase away from the ‘correct phase’ will be kicked out from resonance. The ribbon modes would be partly eliminated by the phase focusing mechanisms, but it is only a few periods for initial electrons to resonate to saturation, hence the electrons still have the probability to survive in the cavity, which results in the degrading of the beam quality in the saturation stage. This kind of suspension behavior will affect the operation of multipacting, thereby affect the quality of electron beams at the gun exit. Fortunately, it is evident that increasing the cavity voltage is a way to eliminate the ribbon modes, hence we will discuss it in MPG.

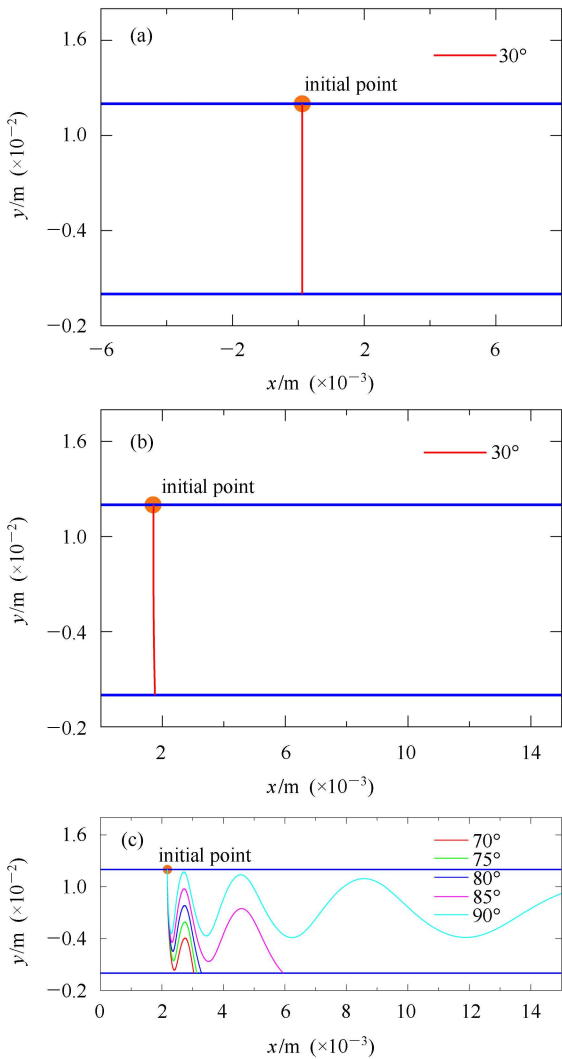


Fig. 7. (color online) The trajectories in the parallel plate for different initial phases and electric fields. (a) and (b) correspond to 9.5 MV/m and 6.4 MV/m maximum electric field in the model respectively; (c) corresponds to 6.8 MV/m maximum electric field.

### 3 Multipacting in the MPG

From the analysis given previously, it seems that the hybrid modes are concurrent in the process of multipacting. For the requirement of high average-current and high-brightness electron beams of the electron gun, it is beneficial to investigate the multipacting effect in the MPG and try to eliminate the effect of ribbon modes, and here we discuss it by constructing a 3-D electron gun model in VORPAL code. Although considering the function of the grid and the characteristics of the cavity shape in the MPG, the results are similar to those we obtained from the parallel plate. A TM<sub>010</sub> RF mode motivated in an S-band standing wave cavity is used to accelerate particles. Further details of the cavity struc-

ture is given in our recent article [18]. The overview of the MPG model is shown in Fig. 8.

With the decision to investigate the effect of cavity voltage, we have initiated studies of the susceptibility area of the multipacting region. The multipacting region, which is divided into the first- and higher order and Ping-pong modes, is shown in Fig. 9. This kind of susceptibility curve of multipacting is used to figure out the design parameters of MPG, such as the gap distance  $D$  and the cavity voltage  $V_{rf0}$ . From the figure here, the rectangle pink area represents the area of  $\delta > 2$ , where  $\delta$  is the secondary emission yield. As the cavity frequency chosen to be a value of 2.856 GHz, the value of  $D$  and

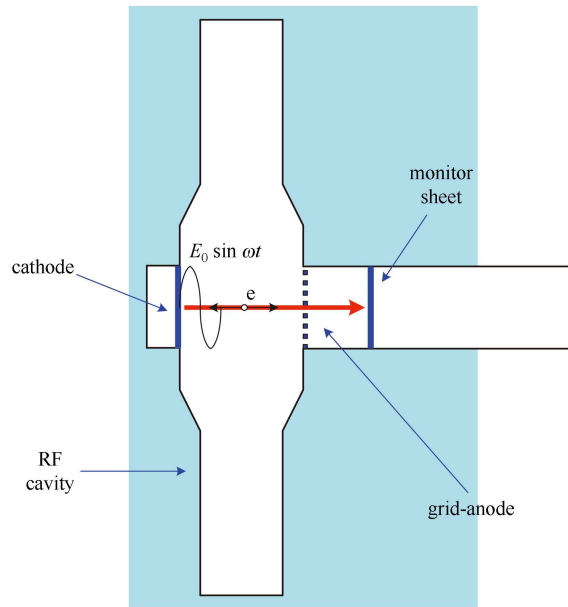


Fig. 8. Schematic of the MPG model.

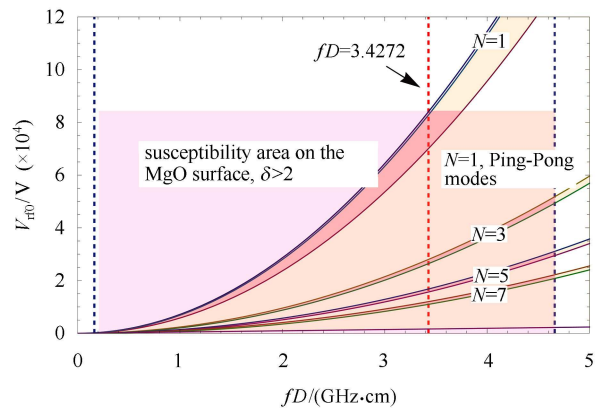


Fig. 9. Susceptibility curve of the hybrid modes.  $N$  is the order of two-surface multipacting and normally we chose  $N=1$  for the gun design. The pink area is the susceptibility area on the material surface which corresponds to the property of the material.

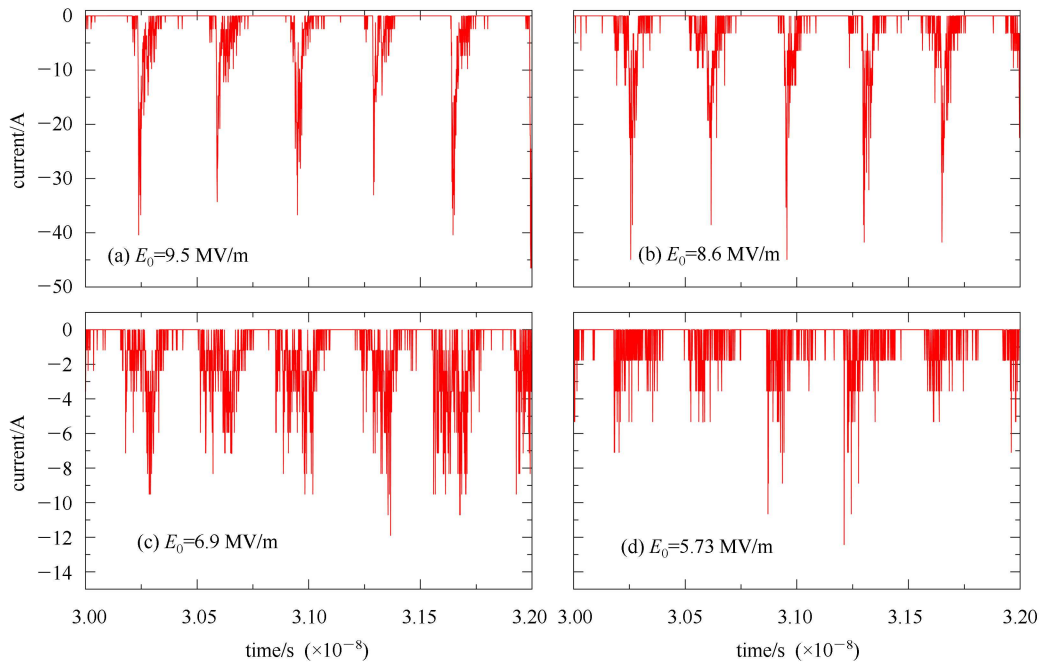


Fig. 10. Micro-pulse structure for different electric fields at saturation stage. The space charge effect was included in this simulations.

$V_{\text{rf0}}$  can be determined from Fig. 9 by confining modes to the 1-st order two-surface multipacting, but discussion of the details is beyond the scope of this paper. Hence we will investigate the effect of cavity voltage by setting the gap distance  $D$  to 1.2 cm. The choice of cavity voltage determines the quality of electron beams, and eventually the power level fed into the cavity.

As a quantifier of beam quality, it is more convenient to evaluate the quality with the bunch length. Fig. 10 shows the micro-pulse structures at saturation for each accelerating field and it is easier to find that the quality of electron beams increases by increasing the cavity voltage. At 5.73 MV/m accelerating field, the resulting beam quality is poor with a bunch length of about 60 percent of RF frequency. The bunch length at 9.5 MV/m accelerating field, which is about 18 ps FWHM, is short enough to be used in the accelerator system. It is important to note that the axis electric field cannot increase infinitely, because it should be confined to within the susceptibility area, which depends on the property of the surface material.

As discussed above, the presence of the space charge effect and ribbon modes are inclined to degrade the beam quality. Hence it is hard to identify the difference between the space charge and ribbon modes from the drawing of Fig. 10. It is clear that increasing the cavity voltage acts to restrain the bunch spread which is caused by the space charge. In order to investigate whether increasing the cavity voltage is a way to eliminate the ribbon modes, a simulation was carried out at the absence of

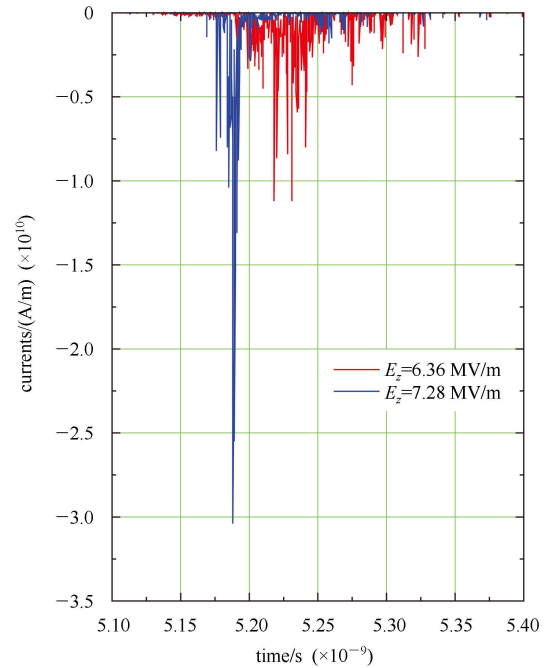


Fig. 11. (color online) Micro-pulse structure for the accelerating electric field at 6.36 MV/m and 7.28 MV/m at the absence of the space charge effect. The simulations here are running for 2-D as compared to Fig. 10.

the space charge effect as shown in Fig. 11, and the figure illustrates the micro-pulse at  $E_z=6.36$  MV/m and  $E_z=7.28$  MV/m. The wide current spectrum at  $E_z=$

6.36 MV/m is rather complicated and is suggested to be occupied by the modes such as ribbon modes. The beam quality at  $E_z=7.28$  MV/m is much better than at  $E_z=6.36$  MV/m at a particular instant of time, from which the spectrum is much more monopolistic. It then allowed us to reach the conclusion that increasing the cavity voltage is a way to eliminate the effect of ribbon modes therefore increase the beam quality. Also from the phase space at saturation as shown in Fig. 12, it is evident that the distribution in Fig. 12 is different from that in Fig. 3. One may conclude that the phase space is changed by increasing the electric field in the cavity so as to eliminate the effect of the ribbon modes and space charge.

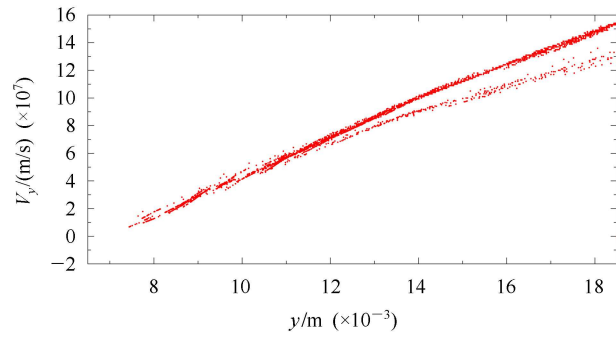


Fig. 12. Velocity in  $y$  direction versus  $y$  when the peak electric field  $E_0=9.5$  MV/m at saturation.

## References

- 1 Farnsworth P T. Journal of The Franklin Institute, 1934, **218**: 411
- 2 Vaughan J M. IEEE Trans. Electron Devices, 1988, **ED-36**: 1172
- 3 Weingarten W. IEEE Trans. Electr. Insul., 1989, **24**: 1005
- 4 Kishek R A. Interaction of Multipactor Discharge and RF Structures (PhD Thesis). University of Michigan, 1997
- 5 Kovalev N F, Nechaev V E, Petelin M I et al. IEEE Trans. Plasma Sci., 1998, **36**: 246
- 6 Sazontov A, Buyanova M, Semenov V, Rakova E, Vdovicheva N et al. Phys. Plasmas, 2005, **12**: 053102
- 7 Slepian J. United States Patent, 1923
- 8 Mako F, Peter W. Proc. 1993 Particle Accelerator Conf., 1993. 2702–2704
- 9 Riyopoulos S, Chernin D, Dialetis D. Phys. Plasmas, 1995, **2**: 3194
- 10 Riyopoulos S. Phys. Plasmas, 1997, **4**: 1448
- 11 Mako F. United States Patent, 2007
- 12 <http://www.txcorp.com>
- 13 Lingwood C J, Burt G, Dexter A C et al. Phys. Plasmas, 2012, **19**: 032106
- 14 Kishek R A. Phys. Rev. Lett., 2012, **108**: 035003
- 15 Agarwal B K. Proc. Roy. Soc., 1958, **71**: 851
- 16 GAO J. Microwave Electron Gun Theory and Experiments, 1991. <http://scitation.aip.org/content/aip/journal/rsi/63/1/10.1063/1.1142680>
- 17 Personal communication (Y. J. Pei).
- 18 LIAO L, ZHANG M et al. Nucl. Instrum. Methods Phys. Res. A, 2013, **729**: 381–386